

WATER MASS TRANSPORT AND HEAT FLUX CHANGES AT 36°N IN THE ATLANTIC OCEAN

by

S.A.Dobroliubov¹, V.P.Tereschenkov² and A.V.Sokov²,

¹Department of Oceanology, Moscow State University, 119899 Moscow, Russia;
e-mail: dobro@ocean.geogr.msu.su

²P.P.Shirshov Institute of Oceanology, Russian Academy of Sciences, 23
Krasikova st., 117851 Moscow, Russia; e-mail: rocc@sovam.com

Abstract

The results of the mass and heat flux comparison at 36°N between 1959, 1981 and 1993 years are discussed. The preliminary analysis of water mass core characteristics (including chemical parameters) revealed the general cooling and freshening at intermediate and deep layers over the entire 34-year period. To estimate the total transport through a plane of a zonal section the technique proposed by Bryan (1962) was used. "Absolute" meridional velocity was assumed to be composed of barotropic velocity, geostrophic velocity and Ekman drift velocity. An integral of each velocity component over the plane of the section was set to zero. The density surface σ_2 separating the Labrador Sea Water (LSW) and the Antarctic Intermediate water (AAIW) was chosen as a "no-motion" level in geostrophic computations.

The barotropic flux (based on the Sverdrup's relation) and Ekman transport were computed using the mean climatic wind stress fields. The results of total mass flux evaluations revealed the intensification of meridional overturning cell in 1981: 21 Sv of southward transport below "no-motion" surface if compared to 14 Sv in 1993 and 9 Sv in 1959. The Gulf Stream transport didn't vary between the cruises. In contrary, the Deep Western Boundary Current (DWBC) transport varied significantly: from 30 Sv in 1959 to 18 Sv in 1981 and to 32 Sv in 1993.

To determine water mass transport the sections were divided into 7 isopycnal layers. The most striking differences in circulation pattern between 1959 and 1981, 1981 and 1993 were observed for LSW and Antarctic Bottom Water (AABW) layers. In contrary to 1959 and 1993, the net transport of LSW ($36.8 < \sigma_2 < 36.94$) and AABW ($\sigma_4 > 45.91$) in 1981 was directed to the north. In 1993 the southward flux of LSW was concentrated both in DWBC and to the west of Mid-Atlantic Ridge, anomalously intensive penetration of Antarctic Bottom Water took place in the Western basin. In addition the 1981 survey was characterised by the reduction of the southward flux of Charlie-Gibbs Fracture Zone Water (GFZW) and intensification of Denmark Strait Overflow Water transport (DSOW).

As a result heat transport through the section in 1981 increased to about 1.3 PWt and was twice higher than in 1959 (0.5 PWt) and in 1993 (0.7 PWt). The dominant part of the total heat flux was determined by baroclinic zonal mean component.

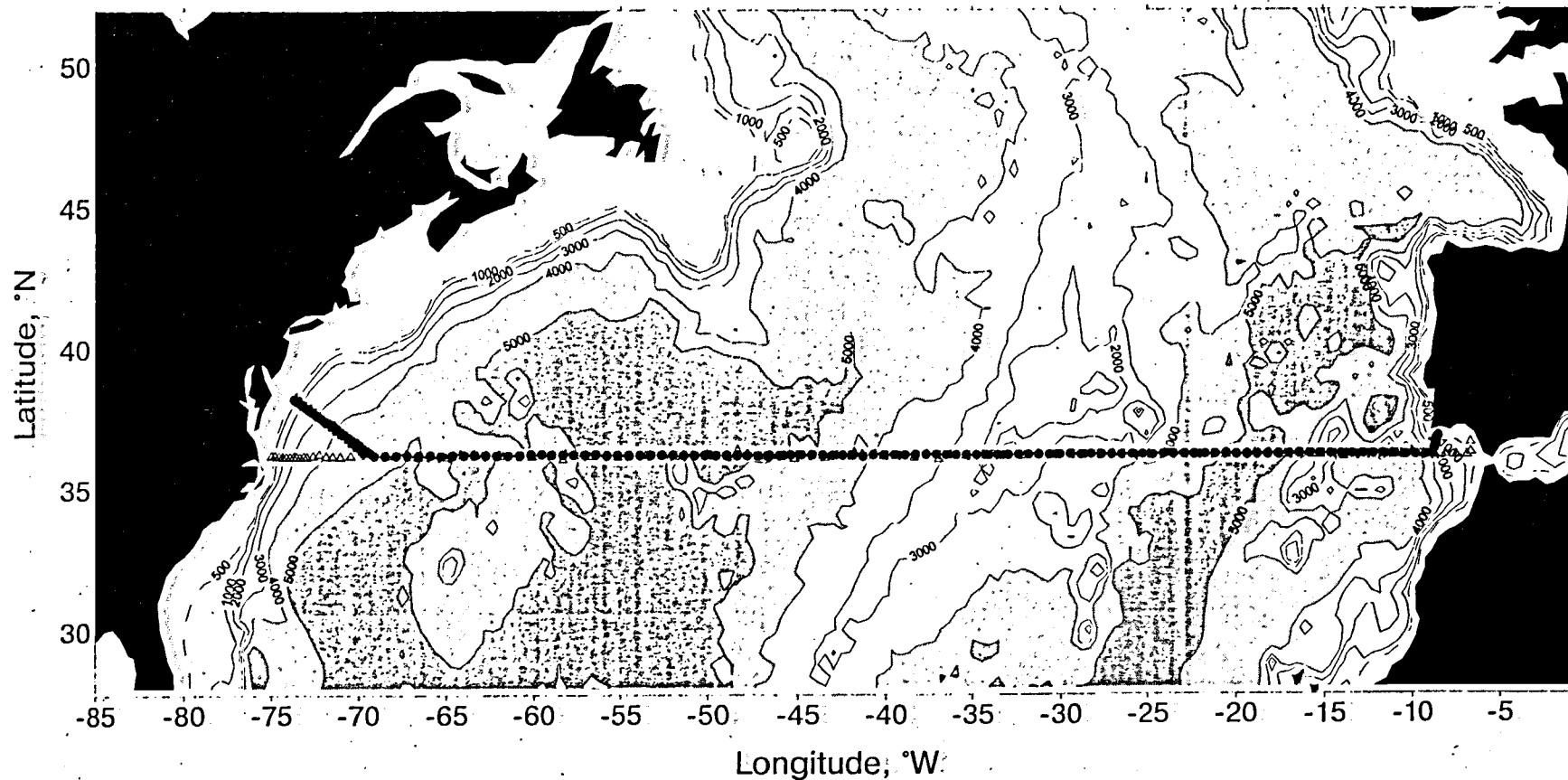


Fig.1 Station position of "Professor Multanovskiy" 1993 (●), "Atlantis-II" 1981 (+) and Chain 1959 (△) cruises.

Introduction

Tereschenkov *et al.* (1995) have reported changes in the thermohaline structure at 36°N in the Atlantic, based on the data collected during three occupations of the ocean-wide hydrographic section by RV *Chain* in 1959, RV *Atlantis-II* in 1981 and RV *Professor Multanovskiy* in 1993 (Fig.1).

Considerable changes in the water mass properties at intermediate and deep layers were reported. In the present study we deal with the estimates of integral properties such as the zonally averaged temperature and salinity and the mass and heat fluxes across the section's plane.

The routes of the three voyages, mentioned above, followed almost the same track except for the western and eastern most parts of the section, but differed in station spatial resolution, specially in the mid-ocean. To greater extent it concerns the 1959 cruise. More to this the 1959 temperature and salinity data has been collected by means of Nansen bottles sampling, while the 1981 and 1993 sections utilised CTD sampling. In contrary to the paper by Dobroliubov *et al.*, (1996), prior to the analyses the data have been rearranged regarding the problem under consideration. For the evaluation of the zonally averaged temperature and salinity differences between the three section repeats all the stations were put on a standard track based on the 1993 survey. The stations were shifted in space in respect to the potential vorticity conservation principle. Than the data were interpolated to fixed spatial grid with 80 km horizontal resolution and 34 vertical pressure levels. The latter were chosen in a way to achieve the best match with the 1959 sampling scheme. For the fluxes evaluation purposes only minor manipulations were applied to the initial data, that have resulted in vertical interpolation of the 1959 data to 20 dbar resolution. In this case all the discrepancies between the cruises were accounted in evaluation of the flux uncertainties. (see Appendixes A,B).

Zonal mean temperature and salinity differences

Fig.2 presents zonally-averaged temperature and salinity differences at 36°N below 500 m. (The surface layers are subjected to strong annual forcing and therefore are characterised by significant annual changes. As far as the sections were occupied in different seasons, the annual cycle obstructed comparison in these layers). The temperature and salinity changes are positively correlated almost through the whole water column, what instantly leads to the tendency of density compensation and to conservation of the water masses density properties. The negative correlation which was observed in some layers for 1993-1981 differences may be related to the changes in the thickness of layers occupied by certain water masses. This argument is confirmed by the significant changes in the depth of "zero" velocity levels, that will be discussed later on. The most significant changes of both temperature and salinity differences are observed in a 800-2200 dbar layer, which corresponds to the distribution of the intermediate waters, specifically to AAIW primarily responsible for the changes in 700-1000 dbar layer and LSW responsible for the changes in 1200-2200 dbar layer. If compared to 1981 a freshening of 0.02-0.03 psu and cooling of 0.1-0.2°C took place. Some smaller negative differences are registered between 1993 and 1959. The cooling up to 0.03-0.05°C is observed also in a deeper layers, but the salinity differences here are not so pronounced if compared to 1981, except for the

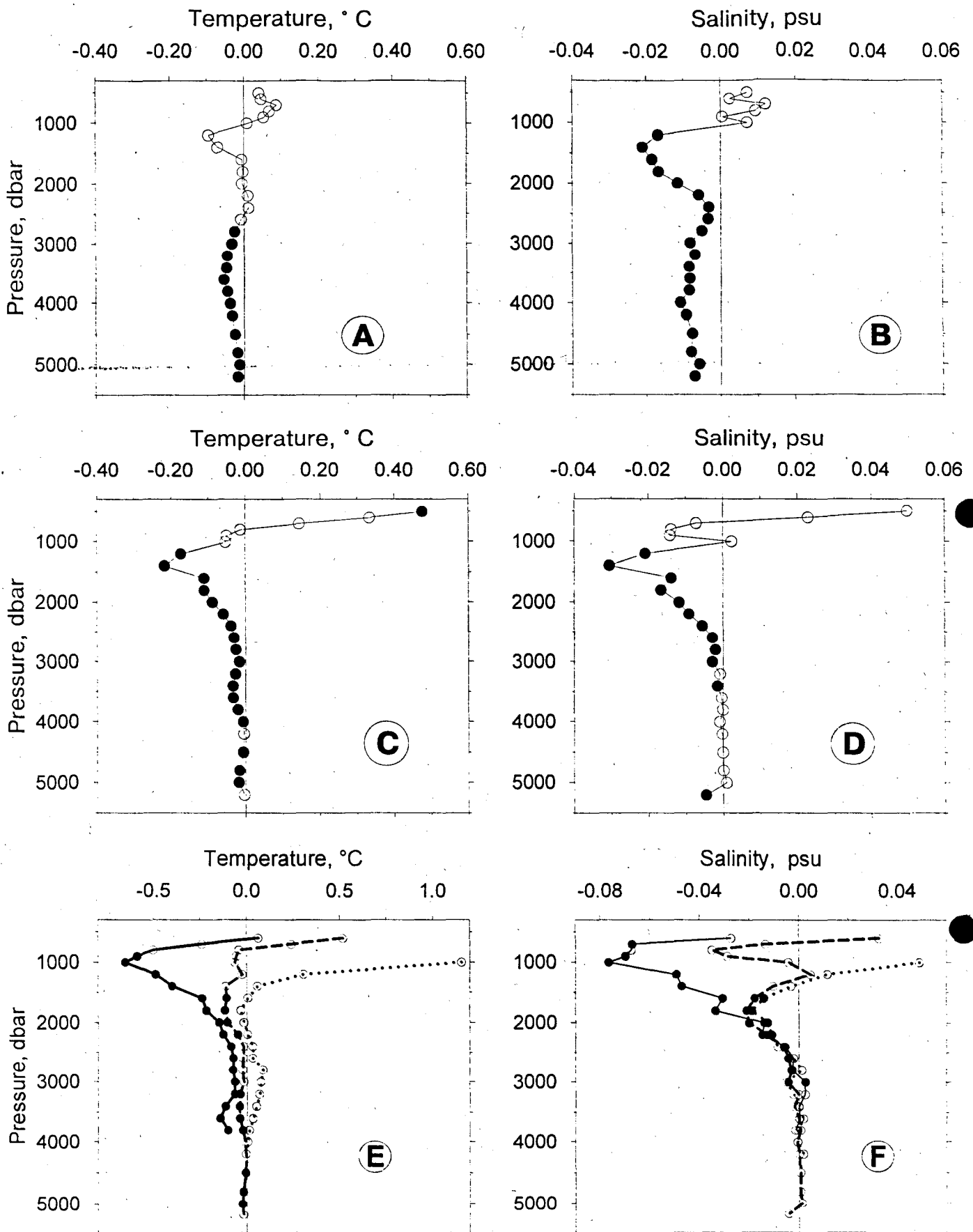


Fig.2 Zonally averaged differences of potential temperature and salinity at fixed pressure levels along 36°N section between 1993-1959 (A,B), 1993-1981 (C,D) for the entire section and for certain parts of the section (E,F): western boundary (····), deep western basin (---) and west slope of Mid-Atlantic Ridge (—). Filled circles stand for the statistically significant values.

remarkable freshening of 0.006 psu that was observed at the bottom layers, occupied by the AABW. Reliability of this freshening is confirmed by the increase in the silicate concentration in these waters. The significant negative salinity anomaly (about 0.01 psu) between 1993 and 1959 is probably due to the salinity problem with the IGY data reported by Mantyla (1994).

It is evident that the zonal mean values are dominated by the characteristics of the mid-ocean, in accordance to the percent of the total section area it occupies. Further on, a more detailed analysis has shown, that the discussed changes in the salinity and temperature structures are seem to originate in the western part of the section (to the west from the Mid-Atlantic Ridge) (Fig.2e,f).

In general the water mass characteristics of the deep waters experienced slight cooling and freshening through the whole period of observations. The intermediate waters became warmer and saltier during 1959-1981 and then cooled and freshened in 1993. It is noticeable that the cooling and freshening in 1993 were more pronounced than preceding warming. Hence, integrally, cooling and freshening took place at the intermediate depth over entire 34-year period.

Water mass transport

The absence of current measurements on the section does not allow to determine the absolute current velocities, and consequently to define the heat and mass fluxes through this latitude. Nevertheless, even the simple indirect methods of the transport estimates for three successive surveys can give an important information concerning the interannual variability of large-scale circulation.

To estimate the total transport through a plane of a zonal section the technique proposed by Bryan (1962) was used. Total meridional velocity is assumed to be a sum of barotropic velocity V_0 , geostrophic velocity V_g and Ekman drift velocity V_e . It was assumed that each of three components of the flow is compensated, so that an integral over the plane of the section equals zero. It means, that barotropic flux, determined from a Svedrup's relation for the eastern and mid-ocean parts of the section, is compensated by barotropic counter flux in the western boundary region. Similarly, Ekman flux in a surface layer is compensated by an equal flux uniformly distributed over the rest of the section area. The balance of the geostrophic flux is achieved by a proper selection of the "no-motion" level.

The analysis of the hydrological structure of waters at the section has shown (Dobroliubov *et al.*, 1995), that water masses formed in the northern parts of the North Atlantic occupied the density interval $\sigma_2 = 36.85-37.09$. It is natural to suggest that at 36°N these waters presumably move southward, away from the source regions. The same considerations bring us to the idea that the flow of the AAIW (occupying the density interval $\sigma_2 = 36.10-36.40$) is directed to the north and Mediterranean water (the density interval $\sigma_2 = 36.40-36.80$) spreads along the 36°N with no distinct meridional component. Therefore it was considered that the "no-motion" level must lie in the density interval $\sigma_2 = 36.70-36.85$. So, as, a first guess, a depth of $\sigma_2 = 36.80$ surface was chosen as a reference level for velocity computations for all three surveys. In the case the sum of the transports above and below the "no-motion" level didn't match, the σ_2 surface was varied until the divergence of the

geostrophic flux equalled to the flow through the Bering Strait (-0.8 Sv). It is interesting to note that the "no-motion" surfaces defined this way differed between cruises rather essentially: from 36.70 in 1993 to 36.73 in 1959 and 36.85 in 1981.

The computations of the barotropic and Ekman components were based on the mean climatic values of the wind stress (Hellerman and Rosenstein, 1983). The Ekman transport at 36°N was estimated to be 2 Sv to the south. The appropriate value of V_e was about -1.0 cm/s at the surface level and less than 0.001 cm/s at underlying levels, regarding the length of the section of 5990 km and the thickness of the Ekman layer of 35 m. Barotropic transport according to Sverdrup relation at 36°N was about 20 Sv (Hellerman, Rosenstein, 1983). The boundaries of the Gulf Stream were set at the stations, between which the total geostrophic transport in the upper 2000 m was directed to the north (Leaman *et. al.*, 1989). The width of the Gulf Stream defined in this manner varied from survey to survey, but at the average was about 250 km. The barotropic additive was 1.5-2 cm/s to the north in the western boundary area and less than 0.01 cm/s to the south in the mid-ocean part of the section.

Fig.3 presents zonally-averaged meridional transport per unit depth at 36°N for the three surveys. Ekman flow was identical in all three cases. Zonally averaged barotropic component was insignificant, though it didn't equal to zero because of the different depth of the western boundary area and the rest of the section. Hence all derived differences are primarily determined by the changes in the thermohaline structure of ocean waters. The depth of the "zero" zonally averaged velocity below the Ekman layer changes from 1100 m in 1959 and 1993 to 1700-2500 m in 1981. Besides the depth of "zero" velocity separating south flowing North Atlantic Deep water and heading north Antarctic Bottom water (AABW) also deepened by about 800 m. In general, northward thermocline water flux (100-1000 m) and southward deep water flux (3200-4500 m) increased in 1981, while intermediate-upper deep water southward movement (1200-3200 m) and northward bottom water transport (below 4000 m) intensified in 1993. Moreover, 1959 and 1993 cruises reflected the pattern with three-layer zonal mean circulation (northward-southward-northward down to the bottom). In 1981 meridional volume flux consisted of only two layers without northward bottom transport.

To obtain more detailed picture of circulation pattern we have divide the zonal section into three main parts: Western boundary (Gulf Stream, slope and shelf regions), Midocean Western (to the west of Mid-Atlantic ridge) and Eastern. In all the regions we have selected 7 density intervals, reflecting the water masses structure. as follows: upper layer water ($\sigma_2 < 36.10$), Antarctic Intermediate water (AAIW: $\sigma_2 = 36.10-36.40$), Mediterranean water (MW: $\sigma_2 = 36.40-36.80$), Labrador Sea water (LSW: $\sigma_2 = 36.80-36.94$), Gibbs Fracture Zone water (GFZW: $\sigma_2 = 36.94-37.04$), Denmark Strait Overflow water (DSOW: $\sigma_2 = 37.04-\sigma_4 = 45.91$) and Antarctic Bottom water (AABW: $\sigma_4 > 45.91$). The total water mass flux at 36°N and through the above mentioned parts of the section together with the uncertainties estimates is presented in Fig. 4. Detailed information concerning the water mass transport calculations and the evaluation of the uncertainties is given in *Appendix A*.

The total water mass transport (Fig. 4a) demonstrated an intensification of upper layer water, MW and DSOW transport in 1981, while LSW and GFZW fluxes were

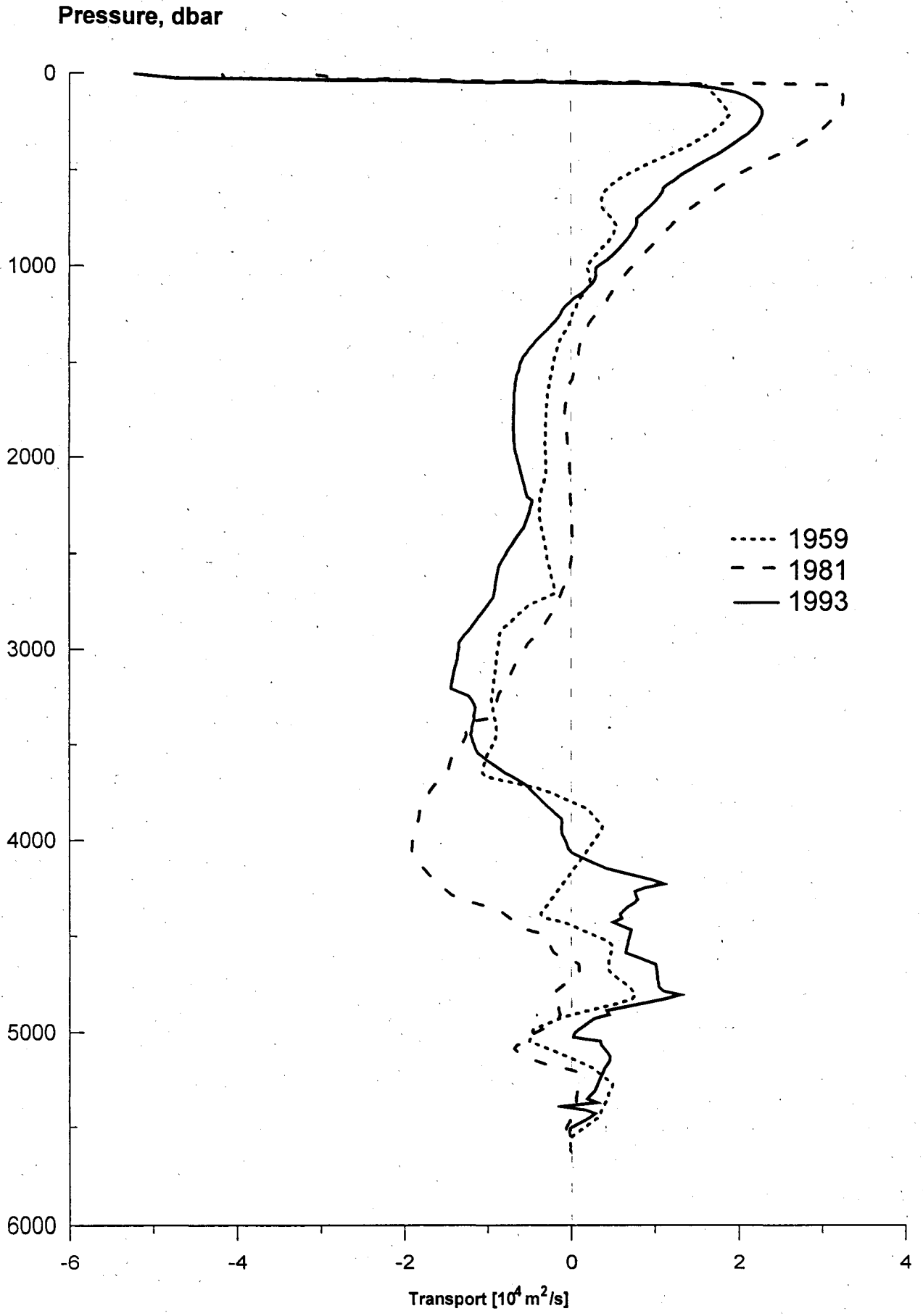
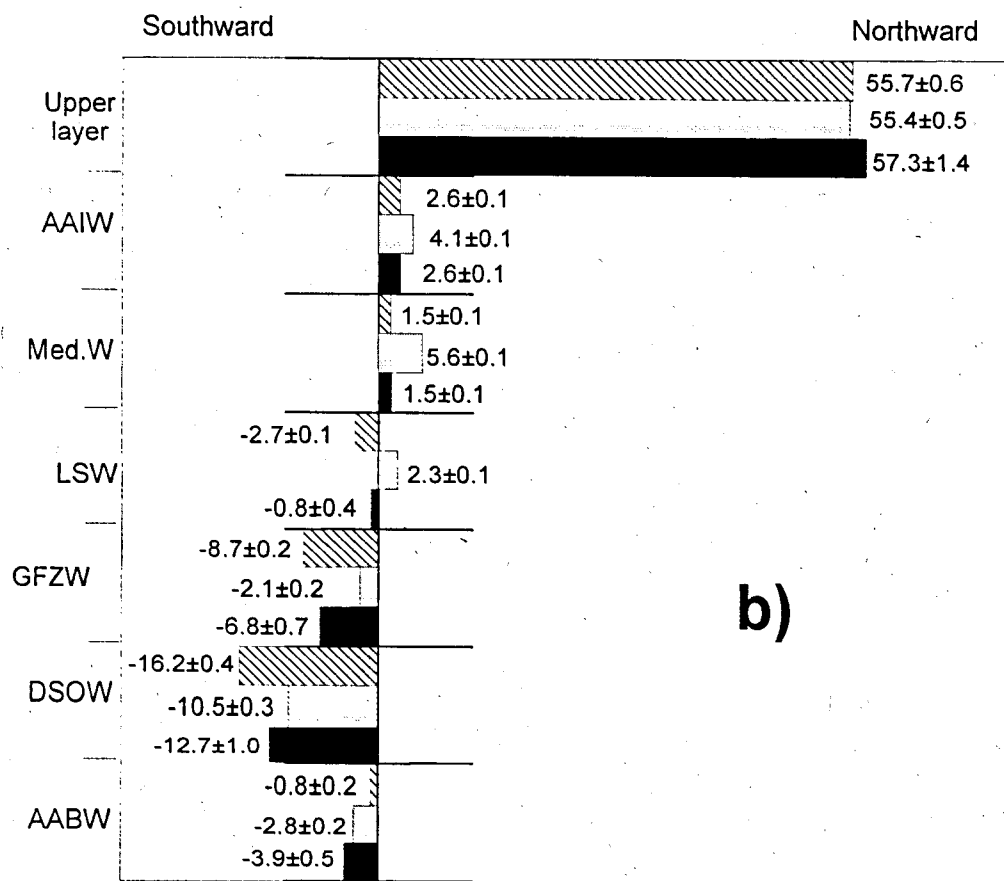
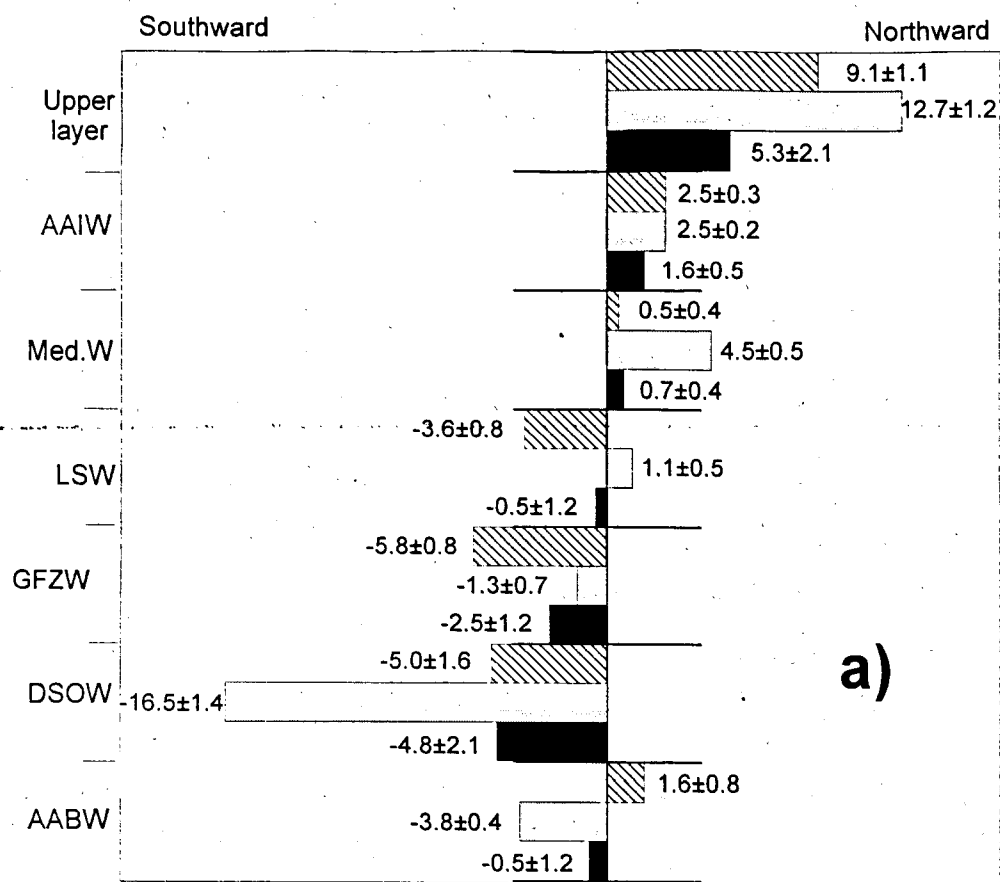
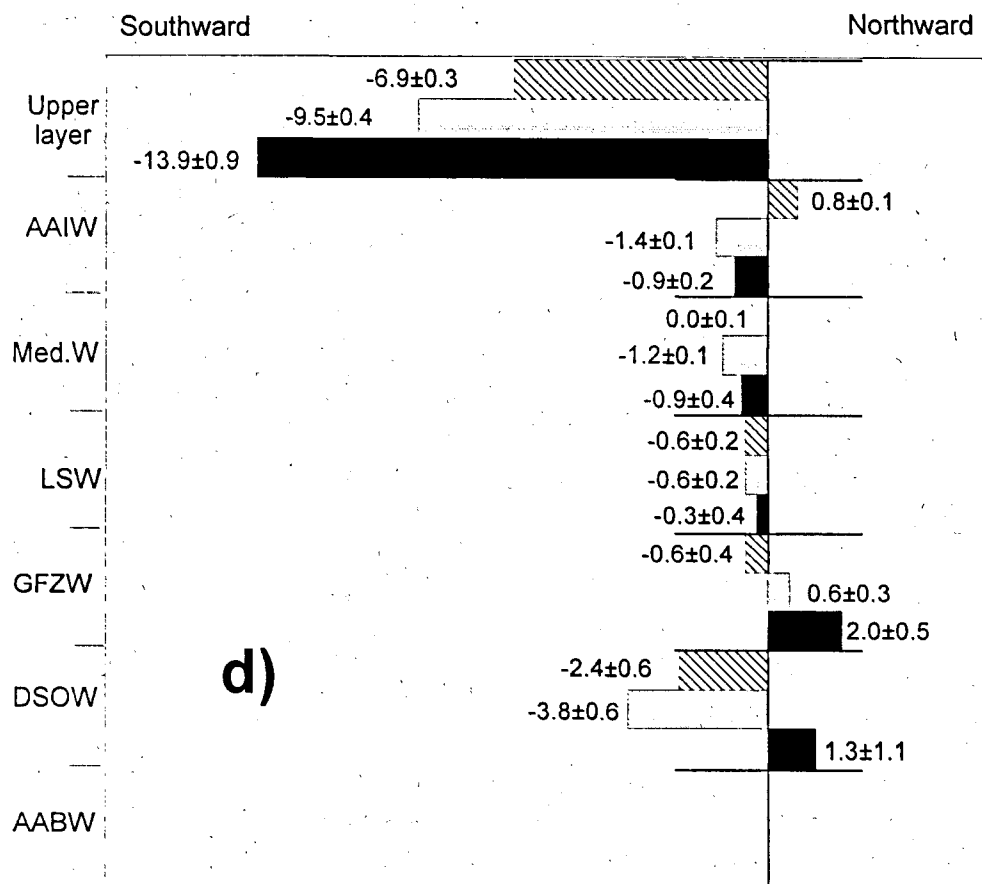
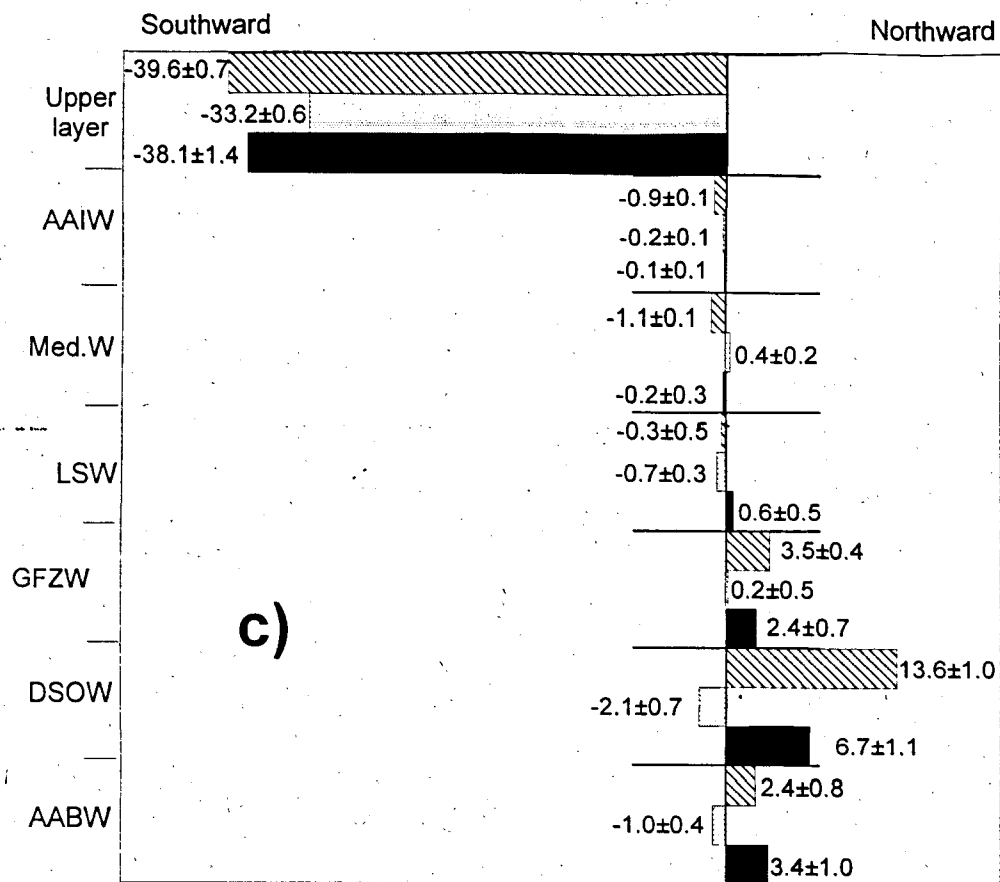


Fig.3 Transport per unit depth for the 36° N section



1959
 1981
 1993

Fig.4. Water mass transport (Sv) at 36 N. a) Total ; b) Western boundary part.



1959
 1981
 1993

Fig. 4. Water mass transport (Sv) at 36 N. c) Midwestern part; d) Eastern part

negligible and AABW flux was directed southward. In 1993 southward transports of LSW and GFZW were of order of 10 Sv, AABW flux was headed northward and DSOW transport was 3-4 times less than in 1981. Water mass fluxes in 1959 revealed the pattern similar to 1993 but were less intensive. In the Western boundary region (Fig. 4b) the upper layer fluxes were the same, the intermediate waters were transported to the north more intensively in 1981 (even in the LSW layer). On the contrary, Deep Western Boundary Current was more intensive in 1993 and 1959. In the Midwestern part (Fig. 4c) upper layer recirculation and northward flow in deep layer (19 Sv) were more pronounced in 1993. In 1981 none of the water masses moved northward in this region (MW northward transport was almost zero). As for the Eastern part of the section (Fig. 4d), the prominent feature was the intensification of the southward upper layer transport in 1959 with counterflux in the deep layers. In 1981 and 1993 the upper layer water mass transport was lower. The manifestation of the changes in the direction of the AAIW flux is supported by the interannual variability of the nutrient concentration in AAIW in the Eastern Basin (Dobroliubov *et al.*, 1995).

Heat flux

In order to evaluate the components of the meridional heat transport (MHT) the method described by Bryan (1962) and Bennett (1978) was used. Barotropic heat transport was computed as the Sverdrup's mass flux times the potential mean temperature difference between the Gulf Stream region and mid-ocean part of the section. Ekman component was determined using temperature difference between upper 35-meter layer and the sectional mean value. This way the heat flux components were computed separately under the condition of no net mass flux through the section; heat transport due to Bering Strait net inflow was suggested to be negligible.

The estimated meridional heat flux during the cruises is represented in table 1, the evaluation of MHT uncertainties is given in *Appendix B*.

Heat flux components at 36°N

Table 1

Year	Component, 10^{15} Watt			
	Barotropic	Ekman	Baroclinic	Total
1959	-0.03±0.04	-0.10±0.06	0.60±0.22	0.47±0.24
1981	-0.04±0.07	-0.13±0.07	1.45±0.14	1.28±0.17
1993	-0.00±0.02	-0.14±0.07	0.84±0.13	0.70±0.15

Variations of barotropic and Ekman fluxes between the surveys are formed by temperature differences because the appropriate volume fluxes are set to be the same. Area-weighted temperature differences between the western boundary region and mid-ocean part were obtained to be relatively small: -0.2-0.6°C. Due to this fact errors in barotropic transport estimation couldn't influence the total MHT. Even if the value obtained from the Sverdrup relation is three times less than the real one (Johns *et al.*, 1995), barotropic MHT would be only of order 0.1 PWt. Ekman heat flux errors are evaluated with 90% confidence probability under the condition of maximum volume flux error of 2 Sv.

Baroclinic (geostrophic) transport was divided into zonal mean, associated with the longitudinally averaged overturning (Bennett, 1978) and horizontal gyre circulation. Evaluated differences between the overturning cell volume fluxes (Fig.3) caused the extremely high changes of baroclinic zonal mean heat transport and consequent increase of total MHT from 0.5 PWt in 1959 to 1.3 PWt in 1981. Similar results were presented by Roemmich and Wunsch (1985). Reduction of total MHT in 1993 is also induced primarily by weakening of vertical overturning cell. It is interesting to note that horizontal gyre flux reflects the simultaneous variations as the zonal mean component.

Conclusions

- Thermohaline structure of the ocean waters at 36°N in the Atlantic experienced significant changes during 1959-1993 time period. The changes effected the properties of intermediate and deep waters of both Arctic-North Atlantic and Antarctic origin. The general tendency was cooling and freshening.
- The core of the "young" LSW was observed in the vicinity of the western flank of the Mid-Atlantic Ridge. What allows to speculate on the existence of a new pathway for the LSW spreading away from the source region.
- The bottom layers cooled and freshened due to the invasion of the AABW
- The most intensive volume transport across 36°N (in a sense of the MOC) was detected in 1981. The changes in the volume transport are primarily induced by the changes in Deep Western Boundary Current region and the pattern of the mid-ocean circulation.
- Meridional heat transport in 1981 was twice higher than in 1959 and 1993.

Acknowledgements

The 40th cruise of RV *Professor Multanovskiy* was supported by the Ministry of Science and Technology Policy of the Russian Federation, the Russian Foundation of Basic Research, and BSH (Hamburg). Scientific analysis of the data was supported under the Grants ISF ME-5000, INTAS-93-2096, RFBR N96-05-65-059 and N96-05-65-061.

References

- Bryan, K., 1962: Measurements of meridional heat transport by ocean currents. *J. Geophys. Res.*, **67**, 3403-3414.
- Bennett A.F., 1978: Poleward Heat Fluxes in Southern Hemisphere Oceans. *J. Phys. Oceanogr.*, **8**, N9, 785-798.
- Dobroliubov, S.A., V.P. Tereschenkov, and A.V. Sokov, 1995: Water mass distribution on 36°N in the Atlantic Ocean in 1993. *Oceanology*, **35**, 6. (In Russian).
- Dobroliubov, S.A., V.P. Tereschenkov, and A.V. Sokov, 1996: Mass and Heat Fluxes at 36°N in the Atlantic: Comparison of 1993, 1981 and 1959 Hydrographic Surveys. *I. WOCE Newslett.*, N 22, 34-37.
- Hellerman, S., and M. Rosenstein, 1983: Normal monthly wind stress over the world ocean with error estimates. *J. Phys. Oceanogr.*, **13**, 1093-1104.
- International Oceanographic Tables, Vol.4, UNESCO, Techn. Pap. Marine Science, 1987, **40**, 195 p.
- Leaman K.D., E. Johns and T. Rossby, 1989: The average Distribution of volume transport and potential vorticity with temperature at three sections across the Gulf Stream. *J. Phys. Oceanogr.*, **19**, N1, 36-51.
- Mantyla A.W., 1994: The treatment of inconsistencies in Atlantic deep water salinity data. *Deep-Sea Res.*, **41**, N9, 1387-1405.
- Johns W.E., Shay T.J., J.M. Bane and D.R. Watts, 1995: Gulf Stream structure, transport and recirculation near 68°W. *J. Geophys. Res.*, **100**, C1, 817-838.
- Rago T.A., Rossby H.T. Heat transport into the North Atlantic ocean north of 32 N Latitude. *J. Phys. Oceanogr.*, 1987, **17**, N 7, p.854-871.
- Roemmich, D., and C. Wunsch, 1985: Two transatlantic sections: meridional circulation and heat flux in the subtropical North Atlantic Ocean. *Deep-Sea Res.*, **32**, 619-664.
- Saunders P.M., 1986. The Accuracy of Measurement of Salinity, Oxygen and Temperature in the Deep Ocean. *J. Physical Oceanogr.*, **16**, N 1, 189-195.
- Tereschenkov, V.P., A.V. Sokov, and S.A. Dobroliubov, 1995: WHP section A3 across 36°N aboard RV *Professor Multanovskiy*. *I. WOCE Newslett.*, N 19, 25-27.

Volume transport estimation errors

It is assumed that the total water mass transport uncertainty in a root-mean-square sense is

$$\Delta Q = (\Delta Q_1^2 + \Delta Q_2^2)^{1/2} \quad (A1)$$

where: ΔQ_1 results from the noise in the thermohaline data and ΔQ_2 is the consequence of mass imbalance and near-bottom velocity uncertainties. In both cases,

$$\Delta Q_{1,2} = \Sigma(\delta V_{1,2} \cdot S + \delta S_{1,2} \cdot V), \quad (A2)$$

where δS is the uncertainty in determination of the area occupied by a certain water mass and δV - shear velocity uncertainty (barotropic velocity was excluded from the consideration).

In order to determine the velocity uncertainty δV_1 related to the errors in temperature and salinity observations the following procedure has been performed. Three sets of 1981 and 1993 CTD data from the Eastern Basin were composed and used for the geostrophic velocity computations. All the CTD profiles were gridded to 20 dbar vertical resolution from the top to the bottom, but the choice of the first pressure level varied for each of the three data sets, particularly 3, 5 and 7 dbar. The r.m.s. deviation between the three derived velocity fields was considered to be the velocity uncertainty δV_1 . In the same manner the velocity uncertainty was determined for every water mass. The maximum uncertainty was defined for the upper layer (≈ 0.2 cm/s). For the bottom layer δV_1 was only 0.1 cm/s. This method could not valid be applied to the 1959 cruise due to the lack of the CTD data. So for the 1959 case we multiplied the δV_1 estimate obtained from 1993 cruise by 4, considering that the IGY data set revealed four times higher r.m.s. deviation of salinity at certain temperature intervals if compared to the CTD data (Saunders, 1986).

It's necessary to bear in mind, that if we integrate $\delta V_1 S$ over several station pairs, the thermohaline "noise" will primarily influence the dynamic height uncertainty δD computed for each station. Mean velocity uncertainty allows to obtain an estimate for the δD :

$$\delta D = (\delta V) / [L \cdot f \cdot (2)^{1/2}], \quad (A3)$$

where L - mean station spacing, f - Coriolis parameter.

While comparing neighbouring station pairs, we can note, that the values of δD for the internal stations compensate each other (assuming that the station spacing, obtained mean noise δD and the water mass layer thickness H are constant):

$$\Sigma V S = \Sigma (H_i \cdot L_i) \cdot (D_i + \delta D_i - D_{i-1} - \delta D_{i-1}) / (L_i \cdot f) = (D_1 + \delta D_1 - \delta D_N - D_N) \cdot H / f \quad (A4)$$

In this case, $\delta V_1 S$ is given by:

$$\delta V_1 S = (2)^{1/2} \cdot H \cdot \delta D / f \quad (A5)$$

If the water mass layer thickness H between the first and the last station pairs varies, A5 must be modified by putting additional term in to it

$$(N)^{1/2} \cdot \Delta H \cdot \delta D / f, \quad (A6)$$

where N - number of station pairs, ΔH - water mass thickness difference. Finally, for $\delta V_1 S$ we have

$$\delta V_1 S = [(2)^{1/2} \cdot H + (N)^{1/2} \cdot \Delta H] \cdot \delta D / f \quad (A7)$$

The uncertainty in the section area is related to the uncertainties in water mass boundary definition. And it is determined as follows:

$$\delta S_1 = \delta p \cdot L \cdot (N)^{1/2}, \quad (A8)$$

where $\delta p = 0.5 \cdot 20m \cdot (2)^{1/2}$ is an error in water mass thickness (for upper and bottom water masses $\delta p = 0.5 \cdot 20m$). Combination of (A6) and (A7) allows to find ΔQ_1 :

$$\Delta Q_1 = S \cdot [(2)^{1/2} \cdot H + (N)^{1/2} \cdot \Delta H] \cdot \delta D / f + \delta p \cdot L \cdot (N)^{1/2} \cdot V \quad (A9)$$

ΔQ_2 is determined as follows. Let's consider that δV_2 accounts for the total volume imbalance δV_{vol} (including Bering Strait transport uncertainty and Ekman flux imbalance) and the uncertainty of the bottom geostrophic velocity determination δV_{bot} . Assuming that the highest possible volume imbalance is about 2 Sverdrups, we estimate the extreme value of δV_{vol} to be 0.008 cm/s. Supposing δV_{vol} to be normally distributed and setting 3σ to be equal to the maximum estimate of δV_{vol} , for the 90% confidence level we get an estimate of δV_{vol} equal to 0.004 cm/s. In order to determine δV_{bot} we used three different ways to define the velocity values in the near bottom triangle V_Δ . The near bottom velocity was derived by extrapolation of the computed velocity values at two deepest levels (h, h-1)

$$V_\Delta = 2 \cdot V_h - V_{h-1} \quad (A10a)$$

or set equal to the deepest calculated velocity

$$V_\Delta = V_h \quad (A10b)$$

or simply set to zero:

$$V_\Delta = 0 \quad (A10c)$$

A10a-A10c result in adding a constant value to the shear velocity in the water column. The maximum additive was 0.02 cm/s; and applying the same considerations as for the δV_{vol} case, we estimate 90% confidence level for δV_{bot} to be 0.013 cm/s. Finally δV_2 is 0.015 cm/s.

We identify δS_2 as an area between the bottom and the deepest levels of observation. This value is about 2% of the total sectional area. The velocity V_Δ

derived from A10a is suggested to be the highest possible value; and A10c condition gives the lowest estimate of the bottom velocity. So we evaluate $V\delta S_2$ as:

$$V\delta S_2 = [\Sigma(0.5 \cdot V_{\Delta} \delta S_2)^2]^{1/2} \quad (A11)$$

$V\delta S_2$ varies from 0.4 Sv in 1981 to 1.3 Sv in 1993 and 1.7 Sv in 1959; it is confined to the water masses which occupy the bottom layers (presumably DSOW and AABW).

The final estimates of the water mass flux uncertainties are presented in tables A1-A3.

Table A1

Water mass transport across the sections at 36°N in 1959

Water masses	SECTIONAL TRANSPORT, Sverdrups						
	Total	American shelf	Gulf Stream	Deep Western	Western slope MAR	Eastern slope MAR	Eastern basin
Upper layer	5.3±2.1	0.0±0.2	57.3±1.4	-33.1±1.2	-5.0±0.6	-5.4±0.5	-8.5±0.8
AAIW	1.6±0.5	0.0±0.0	2.6±0.1	-0.2±0.1	0.1±0.1	-0.5±0.1	-0.4±0.2
Med.W	0.7±0.4	0.1±0.1	1.4±0.1	-0.1±0.2	-0.1±0.2	-0.4±0.2	-0.3±0.3
LSV	-0.5±1.2	2.5±0.3	-3.3±0.3	1.7±0.4	-1.1±0.2	0.1±0.3	-0.4±0.2
GFZW	-2.5±1.2	3.0±0.4	-9.8±0.6	3.8±0.5	-1.4±0.4	1.7±0.3	0.3±0.4
DSOW	4.8±2.1	0.1±0.2	-12.8±0.9	6.1±1.0	0.6±0.5	0.4±0.4	0.9±1.0
AABW	-0.5±1.2	0.0±0.1	-3.9±0.5	3.4±1.0	0	0	0

Table A2

Water mass transport across the sections at 36°N in 1981

Water masses	SECTIONAL TRANSPORT, Sverdrups						
	Total	American shelf	Gulf Stream	Deep Western	Western slope MAR	Eastern slope MAR	Eastern basin
Upper layer	12.7±1.2	2.0±0.1	53.4±0.5	-32.1±0.5	-1.1±0.2	-0.4±0.2	-9.1±0.3
AAIW	2.5±0.2	0.2±0.0	3.9±0.1	-0.6±0.1	0.4±0.0	-0.2±0.0	-1.2±0.1
Med.W	4.5±0.5	0.1±0.1	5.1±0.1	-0.1±0.2	0.5±0.1	-0.6±0.1	-0.6±0.1
LSW	1.1±0.5	0.9±0.1	1.4±0.1	-0.2±0.3	-0.5±0.1	-0.3±0.2	-0.3±0.1
GFZW	-1.3±0.7	2.5±0.2	-4.6±0.1	1.4±0.4	-1.2±0.2	0.4±0.2	0.2±0.2
DSOW	16.5±1.4	0.6±0.2	-11.1±0.2	0.7±0.7	-2.8±0.2	1.2±0.2	-5.0±0.5
AABW	-3.8±0.4	0.0±0.0	-2.8±0.2	-1.0±0.4	0	0	0

Table A3

Water mass transport across the sections at 36°N in 1993

Water masses	SECTIONAL TRANSPORT, Sverdrups						
	Total	American shelf	Gulf Stream	Deep Western	Western slope MAR	Eastern slope MAR	Eastern basin
Upper layer	9.1±1.1	-1.2±0.1	56.9±0.6	-38.4±0.6	-1.2±0.2	-2.8±0.2	-4.1±0.2
AAIW	2.5±0.3	-0.2±0.0	2.8±0.1	-1.2±0.1	0.3±0.1	0.0±0.1	0.8±0.1
Med.W	0.5±0.4	0.0±0.0	1.5±0.0	-0.8±0.1	-0.3±0.1	-0.4±0.1	0.4±0.1
LSV	-3.6±0.8	2.0±0.1	-4.7±0.1	1.4±0.4	-1.7±0.2	0.3±0.1	-0.9±0.2
GFZW	-5.8±0.8	1.9±0.1	-10.6±0.1	5.5±0.3	-2.0±0.3	-0.3±0.3	-0.3±0.2
DSOW	-5.0±1.6	0.3±0.0	-16.5±0.4	14.3±0.9	-0.7±0.3	-1.8±0.2	-0.6±0.6
AABW	1.6±0.8	0	-0.8±0.2	2.4±0.8	0	0	0

Heat transport estimation errors.

The method of "absolute velocity" evaluation allows to separate the total heat transport uncertainty into two parts: "shear flux" uncertainty (baroclinic + Ekman) ΔH_1 and barotropic flux uncertainty ΔH_2 .

1) Baroclinic + Ekman heat flux uncertainty:

$$\Delta H_1 = (a^2 + b^2 + c^2)^{1/2}, \quad (B1)$$

where (Rago, Rossby, 1987):

$$a = \{\delta(\rho c_p)\} \cdot [\Sigma Q \cdot T], \quad (B2)$$

$$b = (\rho c_p) \cdot [\Sigma(\delta Q) \cdot T], \quad (B3)$$

$$c = (\rho c_p) \cdot [\Sigma Q \cdot (\delta T)] \quad (B4)$$

It is assumed that $\delta(\rho c_p)$ equals to the one half of all possible (ρc_p) variations over the sectional area (International oceanographic tables, vol.4, 1987), in this case $a = 0,6\%$ of total heat flux ($a = 0.004$ PWt in 1959 and 1993, 0.008 in 1981).

To compute (B3) we used $\Sigma|\delta Q|$ from the tables A1-A3 and T was defined as velocity-weighted mean water-mass temperature. In this case $b = 0.232$ PWt in 1959, 0.139 PWt in 1981 and 0.149 PWt in 1993.

(B4) can be evaluated as:

$$c = (\rho c_p) \cdot \Sigma(|Q| \cdot \delta T) + Q_e \cdot \delta T_e, \quad (B5)$$

where δT - is the uncertainty of the mean water mass temperature. We estimate δT as a difference between the mean water mass temperature calculated from the data with 20-dbar and 100-dbar vertical resolution. This difference ranges from 0.2° in the upper 1000 m to 0.05° in 1000 - 2000 m and 0.02° below 2000 m. $Q_e \cdot \delta T_e = 2 \cdot 0.5^\circ = 0.005$ PWt, so $c = 0.017$ PWt and $\Delta H_1 = 0.235$ PWt in 1959, 0.159 PWt in 1981 and 0.150 PWt in 1993.

2) Barotropic:

$$\Delta H_2 = (d^2 + e^2 + f^2)^{1/2}, \quad (B6)$$

where

$$d = \delta(\rho c_p) \cdot [Q_{bt} \cdot (\langle T \rangle - T_{GS})], \quad (B7)$$

$$e = (\rho c_p) \cdot [\Sigma(\delta Q_{bt}) \cdot (\langle T \rangle - T_{GS})], \quad (B8)$$

$$f = (\rho c_p) [\Sigma Q_{bt} \cdot \delta(\langle T \rangle - T_{GS})], \quad (B9)$$

where $Q_{bt} = 20$ Sv according to the Sverdrup relation, $\langle T \rangle$ - areal mean temperature at $36^\circ N$ section, T_{GS} - Gulf Stream region mean temperature.

Accounting that the barotropic flux is negligible, $d = 0,6\%$ $H_{bt} = 0$. Even if δQ_{bt} is extremely high (~ 30 Sv - difference between direct measurements and our Gulf

Stream transport calculations), e is only 0.001 PWt in 1993 due to negligible temperature difference ($\langle T \rangle - T_{GS}$) : 0.01° in 1993. During the two other cruises the uncertainty was $e_{1959} = 0.040$ PWt, $e_{1981} = 0.066$ PWt.

If $\delta(\langle T \rangle - T_{GS}) = 0.2^\circ$ - is an error due to the uncertainty of the Gulf Stream boundary determination, than $f = 0.016$ PWt. In this case $\Delta H_2 = 0.043$ PWt in 1959 and 0.068 PWt in 1981 and 0.016 PWt in 1993 (seasonal variability is excluded in this consideration).

Finally uncertainty of heat flux estimation is:

$$\Delta H = (\Delta H_1^2 + \Delta H_2^2)^{1/2} \quad (B10)$$

and equals to 0.24 PWt in 1959, 0.17 PWt in 1981 and 0.15 PWt in 1993.